Contents list available at CBIORE journal website

International Journal of Renewable Energy Development

Journal homepage: https://ijred.cbiore.id

Research Article

Development of a 3D-printed spongy electrode design for microbial fuel cell (MFC) using gyroid lattice

Kristopher Ray Simbulan Pamintuan[a,b*], Harold Octavo Manga[a], Aprilyn J. Balmes[a]

[a]*School of Chemical, Biological, and Materials Engineering and Sciences, Mapúa University, Manila, Philippines*

[b]*Center for Renewable Bioenergy Research, Mapúa University, Manila, Philippines*

Abstract. Microbial fuel cell technology addresses both issues in finding new ways to clean water systems while harnessing electricity. Several studies suggest that a single large-scale MFC is proven to be inefficient and expensive. Therefore, producing small-scale MFCs is focused on investigation to provide an efficient system and cost-effective approach. This study used 3D-printed MFCs using a spongy electrode design to produce a modern approach to modifying electrode capacity in energy generation. Furthermore, the study identifies the electrical conductivity of the spongy electrode by determining the voltage generated and power density by stacked MFCs in series, parallel, and hybrid configurations. The MFCs generate a maximum voltage of 633 mV and a current of 14.22 μA. One way to reduce the effects of voltage reversal in the MFC system is the application of hybrid connection circuits. Parallel-series hybrid connection possesses stable voltage generation of 250−300 mV with the highest current generation of 115.20 μA. At the same time, the Series-Parallel Connection generates the highest voltage and current of 259 mV and 30 μA, respectively. The spongy electrode design and hybrid connection produced a maximum power and current density of 29.30 μW/m^2 and 279.41 μA/m^2 obtained from a different connection of pure parallel and 28P-2S hybrid connection. Furthermore, water quality parameters were examined (pH, TDS, ORP, and COD), that the MFCs design is efficient in wastewater treatment, with a %COD removal of 95.24% efficiency, reduced ORP from +48.00 mV to -7.00 mV, and the TDS concentration from 270 ppm to 239 ppm.

Keywords: 3D-printed electrode, COD removal, gyroid lattice structure, microbial fuel cell, stacking efficiency

Received: 29th Sept 2023; Revised: 15th February 2024; Accepted: 26th March 2024; Available online: 5th April 2024

1. Introduction

The Microbial Fuel Cell (MFC) technology, an emerging alternative technology for renewable energy generation, utilizes living active microorganisms as biocatalysts in anaerobic degradation (Rahimnejad *et al.*, 2015) shows potential in application in wastewater treatment. The anode of the MFC structure is exposed to the wastewater, and the bacteria consumes organic matter from it while producing charged particles by metabolism. The electrons produced from the anodic chamber are accepted by the cathodic chamber while generating electricity (Hadiyanto *et al.* 2023). Bioelectricity generation from investigations in applying MFCs in wastewater treatment has opened studies on different operating conditions to increase its efficiency in removing pollutants, hefty metals, and toxic elements (Habibul *et al.,* 2016; Christwardana *et al,* 2020). However, the electrical performance studies primarily available in its upscaling are still in their infancy. The existing designs of MFCs exhibit low power output wherein composite materials such as carbon nanotubes (CNTs) and carbon-based nano materials (Mustakeem, 2015) as well as fabrication of an assembly of CNT structures were used (Yazdi *et al.*, 2016). The growing 3D printing technology opens an expansive room for design modification and fabrication, particularly in the construction of complex material structures explicitly corresponding to the biocompatibility of the anode since it is exposed to organic materials by design modification, increasing its porosity and surface area. This includes choosing a geometric pattern that would maximize the surface area of the electrode components. A geometric pattern applied for the electrodes in a study in 2021 was a gyroid lattice structure where it exhibited distinctive electrical characteristics due to the pattern's porous nature (Abid *et al.,* 2021) that was deemed favorable to a similar study such as this research.

Electrode material and configuration are also critical to the MFC's performance. The advantages lie in the anode and cathode component's bacterial compatibility, conductivity, surface properties, and costs (Wei *et al.,* 2011). Recent studies show that employing a porous carbon anode improves the power generation of MFC, suggesting its superiority to carbon cloth anode and carbon fiber brush undergoing the same conditions (Bian *et al.,* 2018). Thus, contributing to the further development of studies there is. An innovative way to produce electrode materials to achieve the ideal properties is through additive manufacturing by fused deposition modeling (FDM). This allows profound changes in the material's properties such as freedom of geometrical design, enhanced porosity, and its scaling (Browne *et al.,* 2020). Thus, the capability of producing a complex porous structure reduces the expenses of using ceramic-based or metallic-based electrodes. The use of

* Corresponding author
Email: krspamintuan@mapua.edu.ph (K.R.S.Pamintuan)

https://doi.org/10.61435/ijred.2024.58120
ISSN: 2252-4940/© 2024.The Author(s). Published by CBIORE

conductive polymers in manufacturing electrodes through 3D printing models allows the resolve of the problem of surface-area and electroactive sites available for electron exchange (You *et al.,* 2017)**.** Thus, increasing power output. Conversely, a regular polylactic acid polymer (PLA) was used for the separator of the anode and the cathode. PLAs, as thermoplastic, are among the promising polymers used in 3D printing and are non-electronically conductive (Patrick *et al.,* 2023). Moreover, design modification offers the possibility of commercial use. It examines prospects and challenges for the future of MFC electrode development (e.g., reduction of humanity's dependency on fossil fuels that generate a large amount of greenhouse gases) and ideally helps to mitigate environmental pollutants in wastewater and potentially providing a reliable addition to existing renewable energy sources (Lovley *et al.,* 2011).

The study seeks to develop a spongy or porous 3D-printed electrodes for a multi-celled MFC set-up and determine the effect of stacking these cells in different electrical configurations, series, parallel, and hybrid configurations. Specifically, it aims to analyze the electrical conductivity of the spongy electrode, and determine the voltage generated and power density by the stacked MFCs in series, parallel and series-parallel configurations and compare the results from these configurations among each other; along with analyzing wastewater parameters for testing namely pH, total dissolved solids (TDS), and the oxidation-reduction potential (ORP), and the chemical oxygen demand (COD) reduction to test the wastewater treatment capacity of the design set-up. The application of 3D-printing technology in the production of electrode components appeals to the need for exploratory research on viable designs that would substantially increase power output.

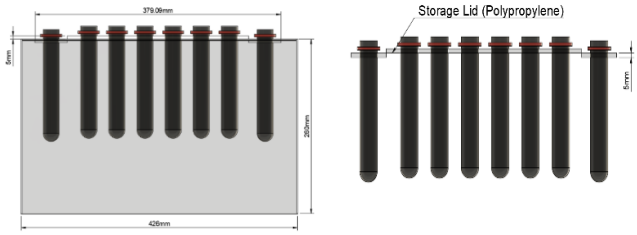

Fig 1. 32 MFC assembly in polypropylene (PP) container

2. Materials and Methods

The experimental setup utilized a 20-liter polypropylene container measured 426 mm x 312 mm x 260 mm (LxWxH) holding the 32 electrodes. 32 holes were made on the lid of the polypropylene container where the outer diameter of the anode was fitted. The electrodes were organized wherein they are

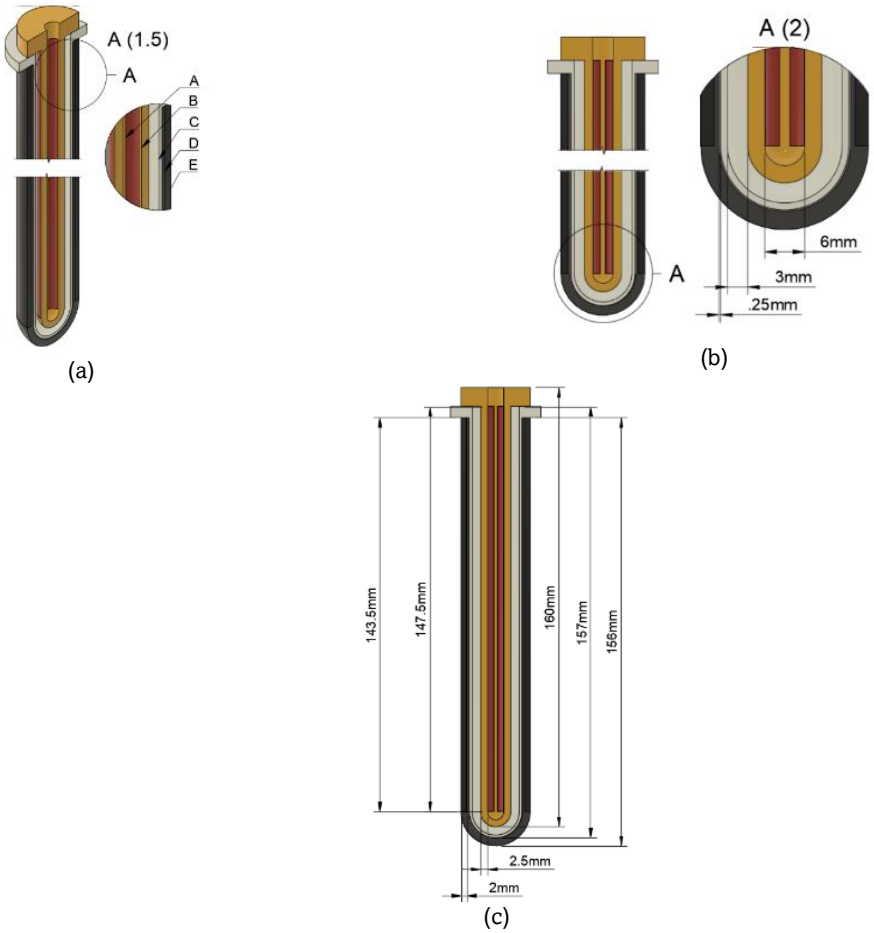

Fig 2. Dimension of the individually fabricated electrodes: (a) electrode sliced perspective; (b) gaps between components; (c) electrode length and thickness

hanging above the lid of the container as shown in Fig. 1 and Fig. 3 where the electrodes can be submerged when the setup is filled with wastewater. The study incorporated a single-chambered MFC of 32-piece stacked electrodes. Fig. 2 shows the dimensions of the individually constructed 3D-printed electrodes.

2.1 Fabrication of 3D-printed electrode

The electrode components were produced through additive manufacturing by a fabrication technique called fused deposition modeling (FDM). The melted polymer filaments were extruded from the nozzle of the 3D-printer building each electrode part layer by layer until the part is completed. All 3D-printed pieces were modeled using a cloud-based 3D modeling software called Autodesk Fusion 360. The design was then imported to a slicing application for 3D printing called Ultimaker Cura wherein the digital designs were decoded by the software into physical dimensions for the 3D printer to read. The design of the 3D-printed electrodes was based on a gyroid lattice structure. With such geometrical complexities, this design pattern for the electrodes was chosen for being highly porous. This allowed optimal bacterial adhesion. This study used a conductive PLA-composite filament (Proto-pasta CDP11720 Electrically Conductive Spool) that was directly bought from ProtoPlant, USA. This was fed to a single extrusion 3D printer machine (Creality Ender-3 V2).

Parts A and B represent the cathode wherein A was a 60% infill gyroid pattern, and B was a 100% infill foundation. Part C is the separator with 100% infill. Part D and E represented the anode where D also had a 100% infill foundation wall, and E had a 60% infill gyroid pattern. Figure 2b shows the gaps between the parts of the electrode assembly. The inside diameter of the cathode was 6 mm, the gap between the cathode and the separator was 3 mm, and the gap between the separator and the anode was 0.25 mm. Lastly, Figure 2c shows the length and thickness of the cathode, the separator, and the anode. The cathode was 2.5 mm thick, while the anode was slightly thicker at 2.5 mm. The length from the upper part of the separator to the 60% gyroid infill was 147.5 mm, while measuring from below was 143.50 mm, giving the thickness of the protruding part of the separator 4mm. The actual lengths of the cathode, separator, and anode are also shown in Figure 2b, 160 mm, 157 mm, and 156 mm, respectively. The gyroid infills in percentage represent the infill density by which the interior volume was set to comprise the material used, specifically the conductive and non-conductive PLA.

The electrode assembly underwent water and resistance tests before the actual experimentation. In this part, rice water was used as wastewater. The permeability of the separator was tested by pouring substantial wastewater into the anode, and the time it takes to drain was observed. This test took

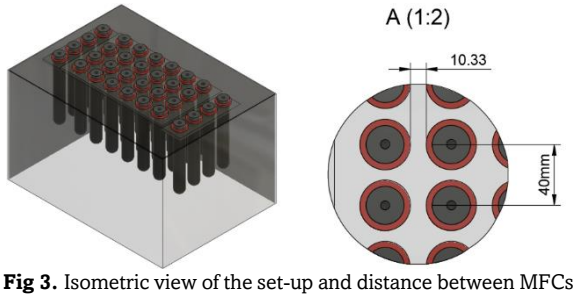

Fig 3. Isometric view of the set-up and distance between MFCs

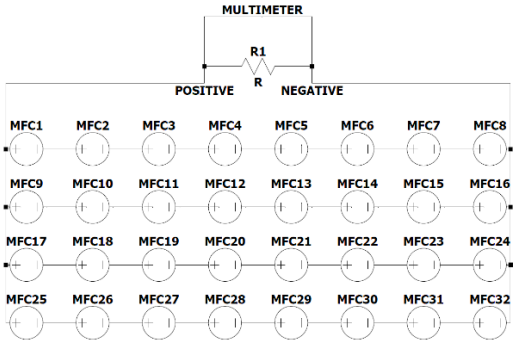

Fig 4. Series-parallel electrical configuration

approximately 4.5 hours for the water to be completely drained. The initial resistance test on the cathode was done using a digital multi-tester), showing a preliminary result of 1.156 kΩ for the cathode and 1.036 kΩ for the anode.

2.2 MFC instrumentation and configuration

The single chamber MFC was operated in a static batch mode for the whole duration of the experimentation. During this, the MFC used the nutrients from the same substrate (wastewater) all through out and the wastewater was not replenished or replaced at any point during the testing period. A multi-parameter water quality monitor pH 117 Multi-parameter Water Quality Monitor) was used to measure water quality indicators such as pH, total dissolved solids (TDS), and the oxidation reduction potential (ORP) every day for two weeks. On the other hand, for the testing of the chemical oxygen demand (COD), the samples taken from the initial and final part of the experiment were sent to a testing laboratory (F.A.S.T Laboratory) in Quezon, City Philippines.

There were various of electrical configurations done throughout the study. The circuits were arranged in series, parallel, and series-parallel configuration, respectively. This was carried out to measure the voltage and current. Cumulative stacking efficiency from previous studies showed a positive impact on increasing the system's and is likely to increase the power and power density of the system. For this paper, the voltages generated were measured against varying external resistances against several electrical configurations. The stacking studies was implemented and explored by stacking studies such as shown in Fig. 4. Moreover, the increase in the number of cells to greater than the usual number of cells (<15 cells) making up an MFC system was also intentionally targeted to achieve a higher power output.

2.3 Sample sourcing and MFC installation

The wastewater sample was collected from a canal greywater reserve in Barangay San Rafael I Sapang Palay, City of San Jose Del Monte Bulacan, in the Philippines. Greywater was considered to be of value to the study since its chemical composition comprised substances such as food fragments, dirt, fats, sludge, or even a detectable amount of feces that may be deemed as a suitable substrate for microorganisms such as bacteria present to metabolize, and thus generate power in the process (Hussain *et al.,* 2022; Sonawane *et al.,* 2022; You *et al.*, 2021). Before using the wastewater sample, parameters such as pH, oxidation-reduction potential (ORP), and total dissolved solids (TDS) were measured using multi-parameter testing equipment (pH 117 Multi-parameter Water Quality Monitor).

The initial chemical oxygen demand (COD) was also measured by laboratory analysis.

2.4 MFC hybrid connection

The voltage (V) and current (I) of the individual electrodes were monitored and measured every three days in terms of the resistances of the MFCs. The cells' cumulative measurements were also measured to determine and make a sufficient comparison between the theoretical and the actual voltage generation of cumulative series and cumulative parallel connections. Since the system is relatively small, at 20 L and with numerous cells (32 MFCs), the conventional testing duration of one month was reduced to a 23-day testing period due to the theoretical assumption that the COD of the system deplete faster in such a scenario. Furthermore, to expand the probabilities of increasing the system's efficiency, stacking studies were performed on the system, such as pure series and pure parallel configurations and a total of 14 hybrid connections of the series-parallel (S-P) connections and the parallel-series (P-S). These are 4S-8P, 8S-4P, 12S-3P, 16S-2P, 20S-2P, 24S-2P, 28S-2P for series-parallel, and the oppositely interchanged connections, which are 4P-8S, 8P-4S, 12P-3S, 16P-2S, 20P-2S, 24P-2S, 28P-2S. This first number corresponded to the number of cells connected in either series or parallel connections, while the second number corresponded to the total number of groups connected in either series or parallel connections. (e.g., 28P-2S hybrid connection means that 28 cells were connected in parallel, and the last four cells out of the 32 were also connected in parallel, giving two groups of cells connected in series).

2.5 Analysis and calculations

The voltage measured using a digital multimeter the voltage reading was used to calculate the current using Ohm's Law, as the power densities, normalized to the estimated surface area of the cathode, and were determined using the formula for calculating current $I = V/R$, and for calculating power density $P = V^2/R$. Where V is the electrode voltage generated, I is the current, R is the electrode's external resistance, and P is the Power density of the MFC.

The measurements for polarization studies were done on the 18th day of the experimentation period from the onset of the submersion of the cell. The first was seven days when the substrate was made to sit for the whole period, considered a pre-colonization stage. The external resistances varied from 16 values, ranging from the lowest resistance of 513 Ω to the highest at 94500 Ω, wherein a potentiometer was utilized. The corresponding voltages were measured along with external resistances set for each reading, where the current was calculated. This allowed the power, power density, and current density calculation, given that the anode surface area is 0.012 m^2. The formulas were as follows: for the calculation of power P=IV; for the calculation of power density PD=P/A; and for the calculation of current density, CD=I/A. P denotes power, I denotes current, V denotes voltage, PD is the MFC's power density, CD is the MFC's current density, and A is the anode's external surface area.

Data for polarization is visualized by generating polarization and power density curves. The polarization and power density curve displayed the voltages and power densities on the y-axis, plotted with the calculated current density on the x-axis. The study mainly showed the power-current-voltage relationship by gradually increasing the resistor load and measuring voltage output with a multimeter. Identifying the highest power/power density value generated by the system allowed the identification of the most efficient current density by which power generation of the cumulative stacking of the 3D-printed electrode is verified. Thus, the development of a more optimized design with reduced internal resistance.

2.6 Chemical oxygen demand removal

Furthermore, a conventional approach will determine the chemical oxygen demand (COD). COD in mg/L was tested in wastewater samples using a laboratory test analysis. Using the equation 1, wherein COD_i and COD_f are the initial and final values, the COD removal efficiency of the MFC stack was calculated.

$$\%COD_{removal} = \frac{COD_i - COD_f}{COD_i} \quad (1)$$

3. Results and Discussion

The spongy microbial fuel cell electrode design was examined for its performance and wastewater compatibility for 23 days. It consists of six tests dedicated to determining the efficiency of the MFCs' performance. The individual performance and resistances of the MFCs regarding voltage and current generation are gathered every three days. It shows the MFC system adaptation to the wastewater system during the exposure of anode to the organic materials inside the system. Studies have shown the ability of utilizing carbon-conductive PLA materials regarding its biocompatibility with organic material (Xie *et al.,* 2011). During the voltage and current measurement, the cumulative cell connection of individual cells was measured to determine and compare actual voltage generation of MFCs.

Moreover, the hybrid configuration of MFCs was conducted to establish the stacking capabilities of the designed 3D-printed electrode assembly. Along with these stages of trials, the power and power density of the electrode hybrid configuration was identified as well, together with its polarization curves, allowing the direct observation of the performance of the MFC system configuration (Simeon *et al.,* 2020), with connections such as 4S-8P, 8S-4P, 12S-3P, 16S-2P, 20S-2P, 24S-2P, 28S-2P, for series-parallel connection and pure series connection. Alternately, for the parallel-series connection, it was imparted to conduct the interchangeable configuration, such as 4P-8S, 8P-4S, 12P-3S, 16P-2S, 20P-2S, 24P-2S, 28P-2S, and pure parallel connection. Ultimately, the external resistances of these connections and the design attributes of the 3D-printed spongy electrode were measured, which determines the circuit regulation of electron flux and the MFC's anode availability as an electron acceptor (Jung & Regan, 2011). The wastewater quality parameters were limited to four assessments: the treatment stage and data collection for pH, Oxidation Reduction Potential (ORP), and Total Dissolved Solids (TDS) lasted for two and a half weeks, while the Chemical Oxygen Demand (COD) took approximately three weeks of data acquisition.

3.1 Individual voltage and current reading of 3D-printed spongy Microbial Fuel Cell

The final voltage readings of 32 individual cells are shown in Figure 5. It is observed that the voltage readings are different from the pre-colonial stage voltage reading and the post-treatment stage voltage reading. The inconsistent reading of voltage generation for the individual cells was observed due to

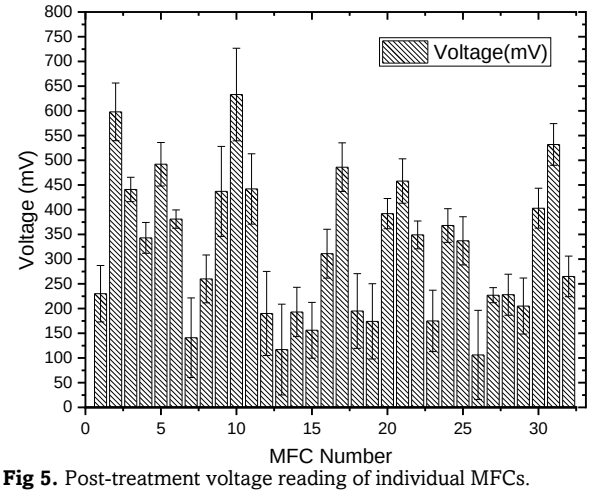

Fig 5. Post-treatment voltage reading of individual MFCs.

different overall resistance values measured of individual MFC that are caused by the 3D-print quality of each cell, which affects the capacity MFC to generate voltage. The individual electrodes such as anode and cathode are produced in batches. This process creates a difference in internal resistance which is caused by the difference in characteristics such as print infill affecting the overall performance of each MFC.

Moreover, the generated voltage for each cell during the pre-colonial stage of biological content in the MFC system varies due to the difference in bacterial species. Therefore, the activity of the species affects their adaptation to one another and to the material that contributes significantly to the transfer of electrons during bacterial growth (Daniel *et al.,* 2009; Hashem, 2019; Jung & Regan, 2011). The MFC chamber's setup is designed to be anaerobic, promoting the growth of electroactive bacteria (EAB). Several types of EAB commonly grow without oxygen. These bacteria are obliged anaerobes since their energies are generated from metabolic processes that do not utilize oxygen from their surroundings.

The 3D-printed MFCs in this study possess a general concept of how individual microbial fuel cells are expected to generate energy. The bacteria in the anodic side of the electrode create a biofilm that serves as the bacterial adaptation for the MFCs. Thus, the substrate began to oxidize while the system was anaerobic. From there, it releases electrons to the anode, which is transported to the cathode side through the proton exchange membrane that acts as a separator with a Polylactic acid (PLA) material that somewhat allows the transfer of particles to the cathode side of the cell. This phenomenon of electron transfer through a membrane to the cathode generates electricity through the external circuit, observed in the voltage reading of individual MFCs. This data proves that the electroactive bacteria accepted the MFCs 3D-printed design, which is expected to generate significant voltage through the treatment period. The determination on day 23 of the wastewater treatment shows that in 3 weeks, the individual cells increased their voltage generation, and only nine cells decreased their voltage generation from the initial to the final treatment from the 32 sets of individual cells. Referring to Figure 5. (Day 23 Data), the cells with significant voltage are MFC2, MFC5, MFC10, MFC17, and MFC31. These MFCs generate a voltage of approximately 500 mV during the final treatment period.

Furthermore, the designed anode has a calculated external surface area of 0.012 m^2, used to determine the power and current density of the MFC system for the pure and hybrid connections. The individual MFC voltage reading is very similar to studies using 3D-printed MFCs. The monolithic design of MFCs using conductive PLA generates a voltage generation range of 480 to 500 mV. Furthermore, some findings acquire open circuit potential (OCP) of 116 mV using the conductive filament produced by Additive Layer Manufacturing of cathode MFC electrode (You *et al.,* 2017). Additional studies that use 3D-printed porous copper electrode has a maximum voltage of 62.9 ±2.54 mV. Somehow, the 3D-printed MFCs using Carbon for anode material produce a significant amount of maximum voltage of 453.4 ±6.5 mV (Bian *et al.*, 2018) These suggest that the spongy electrode 3D design significantly impacts the voltage generation of the MFC wastewater system.

3.2 Series and Parallel MFC circuit connection

The individual cell voltage and current generation, the pure series, and the pure parallel connection are initiated to determine the efficiencies of different configurations among the MFCs and conclude a more comprehensive study regarding optimizing the power output of MFCs. Studies show that series and parallel connections are significantly different in the large-scale system of MFC technology. The phenomenon that affects the performance of MFCs is the voltage reversal generated by the circuit. The stacked MFCs create a voltage drop, producing a negative voltage reading under short-circuit conditions. Another observation during this phenomenon is that the difference in voltage output while connecting MFCs has different spikes of voltage drop and voltage rise. This is due to the substrate loading rate resulting in inactive kinetics on the anode and generating a relatively large anode overpotential much greater than the cathode (An *et al.*, 2016). One of the notable adverse effects of voltage reversal is its power generation throughout the treatment period of the wastewater system.

Furthermore, voltage reversal has a crucial dissociation effect on the anode biofilm that could potentially alter the efficiency of individual MFCs. The voltage reversal of circuits is observed more in the series connection since the individual fuel cells acquire internal resistance differences that affect the current between MFCs connected in a series configuration (Chang *et al.,* 2020). Furthermore, the parallel connection observed a significant voltage generation compared to a series connection that prevents large voltage loss during the testing of pure parallel connected MFCs.

3.3. Cumulative Stacking of Series and Parallel Circuit Connection

In MFC research, the stacking of MFCs has been growing interest to develop the system's wastewater treatment efficiency and power generation. However, there are numerous methods of connection that can be applied, which need to be considered. Figures 6 and 7 are the results collected in 2 weeks of wastewater treatment for the cumulative stacking of series and parallel circuit connection. The series circuit connection, shown in Figure 6, generates a large gap between the theoretical and actual voltage readings. From a theoretical perspective, a series connection will generate proportional growth in voltage generation. However, in the real-life application of a series circuit connection of an MFC system, there is significant voltage loss during the treatment and observed in different literature investigating MFC in other configuration connections. As stated, this is due to the voltage reversal caused by the difference in voltage generation of individual MFCs when they undergo large quantities of connected cells (Gajda *et al.*, 2018). The largest voltage generation for the cumulative series

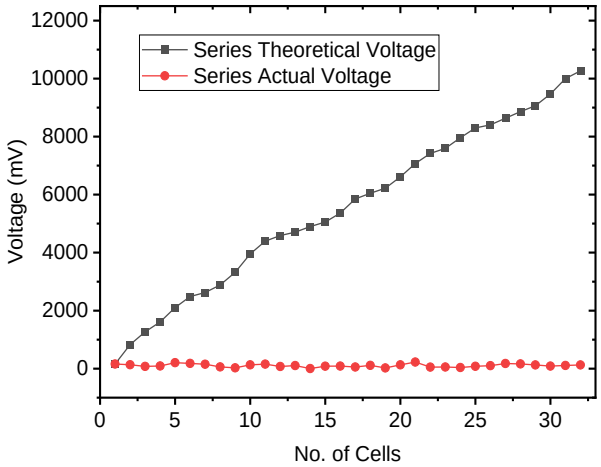

Fig 6. Cumulative stacking of pure series connection; theoretical and actual voltage reading

connection was produced by MFC21, which generated a maximum voltage of 226.45 mV.

Furthermore, the parallel cumulative circuit connection in Figure 7 reveals a different voltage generation; it produces better voltage generation than a series circuit connection. The theoretical voltage reading and the actual voltage reading are different in the initial stage of MFC treatment. However, the theoretical and actual reading begins to produce the same values in the latter part of the treatment. These results prove the conceptual effects of stacking multiple MFCs: voltage stables in an average amount and current increases as the wastewater treatment progresses (Jafary *et al.,* 2013). Regarding the internal resistance of the 3D printed electrode, individual MFCs for the anode have an average internal resistance of 0.78 Ω, while the cathode has an average internal resistance of 1.50 Ω. This suggests that the resistance for the electrolytes from the substrate was low, which possesses a better flow of electrolytic particles through the MFCs. Developing new designs for the MFCs creates more optimization for MFC modification. The voltage response produced in stacked MFCs connected in series shows the same behavior from previous Voltage Reversals (VR) investigations on MFCs. Thus, this limits the performance of the MFC system. However, this can be mitigated by several approaches to the circuitry and the substrate quality used during wastewater treatment. One of the solutions to avoid VR is to eliminate the individual cell with low voltage generation. However, this has implications in the system of multiple MFCs. In that notion, it is practical to apply hybrid connections in each MFC to overcome the loss of voltage and current. Another method can be used by modifying the system and quickly short-circuiting that, generating a voltage drop during the trial period. One way to achieve this is to use diodes connected in the circuit due to the diode's low ohmic resistance that prevents charge reversal. This will enhance the capacity of the system to short-circuit individual cells with less modification on MFC design automatically. Ultimately, focusing on the structure of the MFC can also help avoid VR by increasing the concentration of the substrate and allowing more oxygen to the cathode side of the MFC. It will prevent the fuel starvation of the microorganism inside the system and the process of continuous treatment operation (Oh & Logan, 2007).

3.4. MFCs Stacking Combinations

The stacks and controls of the pure connections of series and parallel circuits were discovered to have different behaviors during the trial period of the wastewater treatment. The pure series connection creates unstable voltage generation caused by voltage reversals of the circuit while increasing the number of connected cells. Furthermore, the cumulative parallel circuit was observed to suffer from energy loss due to the nature of the MFC system itself. Several factors might affect this phenomenon in this type of system, mainly because it relies on the biological activity of microorganisms inside the MFC chambers or systems, electrolytic resistance losses in electrodes, potential losses in both anode and cathode chambers, and the type of electrical circuit used, whether it is running under an open or closed circuit (Kim *et al.,* 2011).

3.4.1 Stacking Combination of Series-Parallel Hybrid Connection

The stacking combination of series-parallel connection was conducted seven days after the pre-colonization stage of the biological matter in the wastewater system; at this point of treatment, the biofilms are established to optimally generate substantial energy and power, individually and in circuit connection (Alonso-Lemus *et al.,* 2022; Yanuka-Golub *et al.,* 2021). From Figure 8, it is observed that the voltage generated by hybrid connections possesses a unique output. However, the trends produced by the series-parallel circuit allow the system to generate significant voltage and observe the current difference. The data shows that the current generation

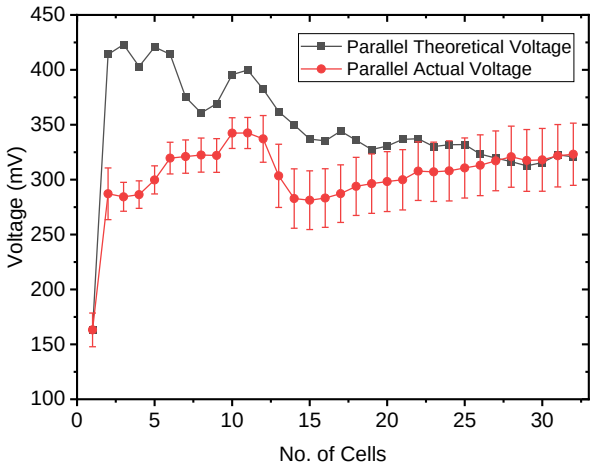

Fig 7. Cumulative stacking of pure parallel connection; theoretical and actual voltage reading

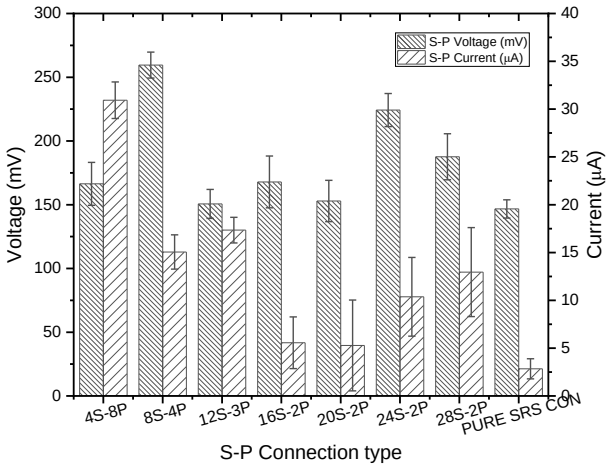

Fig 8. Cumulative series-parallel hybrid connection voltage and current reading

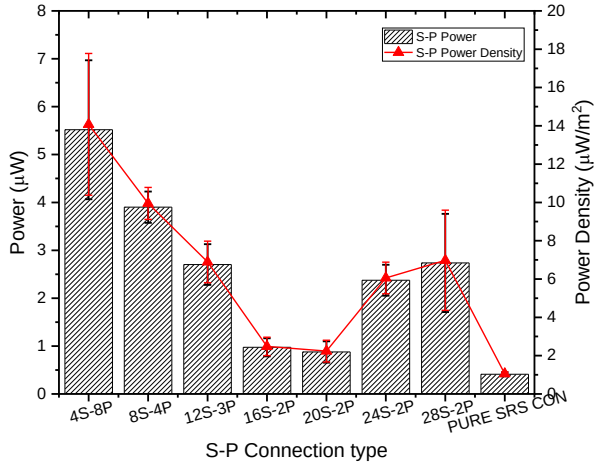

Fig 9. Cumulative series-parallel hybrid connection; power and power density reading.

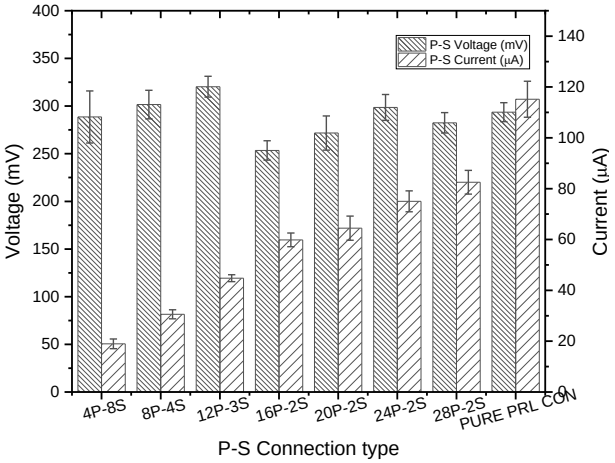

Fig 10. Cumulative parallel-series hybrid connection; voltage and current reading

decreases for the 7-day trial period as the series connection increases. Incorporating a cumulative combination of stacked Series-Parallel MFCs offers enhanced performance of the whole wastewater treatment. Additionally, the hybrid connection that generated a significant result was 8S-4P and 24S-2P, which generated a voltage of 259.57 mV and 224.28 mV and a current of 15.06 μA and 10.37 μA, respectively. The hybrid connection maintained the relative increase of power density and the connection's power generation.

Figure 9 shows the cumulative series-parallel hybrid connection's power and power density, resulting in a decreasing value trend. This indicates that as the series connection increases and the connected group of series connected in parallel decreases, it produces a lower power generation and power density of hybrid connection. These results indicate that the most efficient connection has fewer MFCs connected in series, producing a more significant number of cell groups to be connected in parallel. Furthermore, connections that reveal the significant power and power density are 4S-8P, 8S-4P, and 12S-3P, which produce a maximum value of 5.52 μW, 3.90 μW, and 2.70 μW for power. With power densities of 14.07 μW/m^2, 9.95 μW/m^2, and 6.89 μW/m^2, respectively. Consequently, the increasing number of connected cells in series generates a limited power and power density. Hybrid connections such as 16S-2P, 20S-2P, and pure series connections generated 0.97 μW, 0.88 μW, and 0.41 μW, respectively, reflected by the voltage and current generation.

3.4.2 Stacking combination of parallel-series hybrid connection

The parallel-series connection significantly increases voltage and current generation, as shown in Figure 10. The results show that even if the number of connected parallel MFCs increases, the voltage still produces an average value of 288.77 mV. Significantly, hybrid connection 12P-3S has the highest voltage of 320.28 mV. Moreover, the hybrid connection reveals a different view of how stacked MFCs generate current in these configurations. Figure 10 also shows that as the connection of MFCs in parallel increases, the current generation also increases. The pure parallel connection found that it has the highest current generation of 115.2 μA and has 4P-8S with the less efficient hybrid parallel-series connection that only produces 18.97 μA. These results also reflect the studies of bioelectronics platforms possessing current loss. One of the analyses of hybrid connections is that stacked parallel-series MFCs decrease the possibility of voltage reversal (An *et al.*, 2016). However, a large number of unit cells stacked in more parallel groups connected in series results in inner-circuit current loss, also called current reversal (Wu *et al.*, 2016).

The power and power density efficiency of parallel-series hybrid connections significantly differ from the series-parallel hybrid connection. The same trend was revealed: power and power density also increase as hybrid systems' parallel connection increases. This is reflected in the current generation's increase as the connection of MFCs forms a pure parallel connection with hybrid connection 4P-8S possessing the least power of 5.70 μW leading up to the most significant generated power of 34.04 μW on the pure parallel MFC connection. The whole trial period suggests that both series-parallel and parallel-series connection have their strengths and weaknesses regarding power, voltage, and current generation. Several studies were recorded to achieve a peak of power generated in the system of 0.92 μW to 11.39 μW**.** The material used in the study was a Polylactic Acid Filament (PLA) that produces 3D-printed MFC components of the MFCs. This signifies that the complexity of the design has contributed to generating a much more efficient power generation.

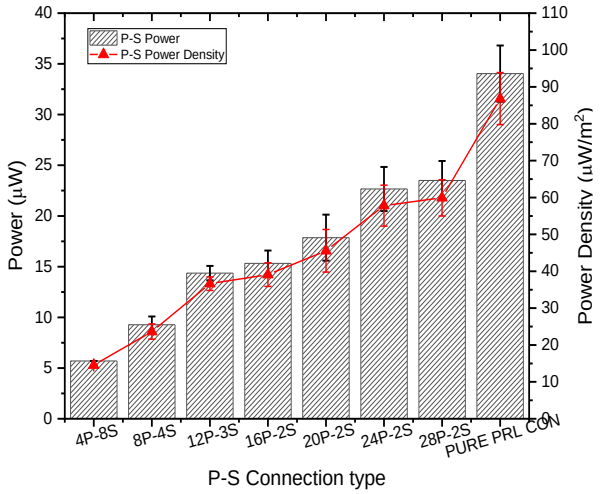

Fig 11. Cumulative parallel-series hybrid connection; power and power density reading.

Table 1
Polarization data for cumulative stacking of MFC pure and hybrid connection

Hybrid MFC connection code	Maximum External Resistance (mΩ)	Maximum Power (μW)	Maximum Power Density (μW/m²)
Series – Parallel Hybrid configuration			
4S-8P	3.37	9.86	25.15
8S-4P	15.00	2.38	6.09
12S-3P	7.30	2.73	6.97
16S-2P	25.40	1.29	3.30
20S-2P	15.00	1.29	3.30
24S-2P	15.00	1.15	2.95
28S-2P	10.05	3.33	8.50
Pure Series	25.40	0.56	1.45
Parallel – Series Hybrid Configuration			
4P-8S	15.00	2.66	6.80
8P-4S	7.30	3.62	9.24
12P-3S	2.02	4.71	12.02
16P-2S	2.48	4.85	12.37
20P-2S	3.37	5.44	13.87
24P-2S	1.37	7.65	19.53
28P-2S	0.62	7.41	18.91
Pure Parallel	1.37	11.48	29.29

3.5 Polarization curve of pure and hybrid connection

This study section shows polarization studies, one of the most common fuel cell testing methods. Using a potentiometer, the resistance load was increased from 0.513 kΩ to 94.5 kΩ, and by using the measured surface area of the electrode being 0.012 m², the voltage response was recorded wherein Ohm's Law determined the corresponding current values along with the power and power densities calculation.

The pure series and series-parallel configurations shown in Table 1 show the polarization data of the pure series and the series-parallel configurations. There are seven hybrid series-parallel configurations, which are 4S-8P, 8S-4P, 12S-3P, 16S-2P, 20S-2P, 24S-2P, and 28S-2P. The y-axis denotes the power generated in microwatts, while the x-axis represents the current in microamperes. The maximum power generated is attributed to the graph's peak concerning its corresponding most efficient current density.

Comparing the results in both sections, the peak power generation for the gyroid-lattice structured MFC system is at 11.49 μW with a current value of 91.60 μA from the pure parallel configuration against an external resistance of 1369 Ω. This is summarized and shown in Figure 12, with the voltage readings and power densities plotted on the x-axis against the current densities plotted on the y-axis. The polarization line of voltage is plotted along with the current density and power density, which both consider the electrode's surface area being 0.01225 m², by which the maximum power density is at 29.29 μW/m². Moreover, the lowest power generated is by the pure series configuration at 0.57 μW, having a lower current value of 4.74 μA against an external resistance of 25400 Ω. Power densities increase to a peak point and then deteriorate after a duration. This result trend ties nicely with the typical polarization and power density graph wherein the cell voltage decreases with an increasing current density by Ohm's law. Moreover, it shows the power density relationship with the current density. The external resistance of the purely parallel stacked cells at 1369 Ω attaining the maximum power achieved can also be attributed to the cells' total internal resistance in the polarization studies

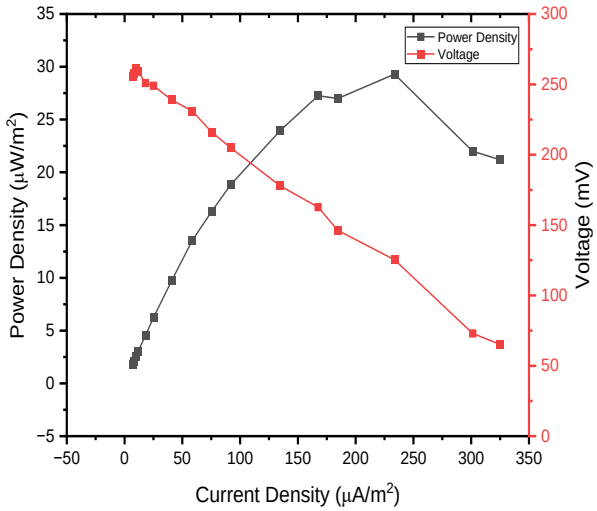

Fig 12. Maximum polarization and power density curve for cumulative pure parallel connection

(Logan *et al.,* 2006). Herein, the external resistance would be equivalent to the internal resistance.

3.6 Wastewater treatment parameter reading

Several wastewater parameters were part of analyzing the functioning 32-celled microbial fuel cell system. This includes the oxidation-reduction potential (ORP), the total dissolved solids (TDS), pH, and the chemical oxygen demand (COD) removal. The application of the MFC system was not limited to power generation, but several studies have explored its functions using several wastewater types.

The oxidation-reduction potential of the system after 15 days (about two weeks) was observed to have linearly decreased, as well as the system's total dissolved solids (TDS).

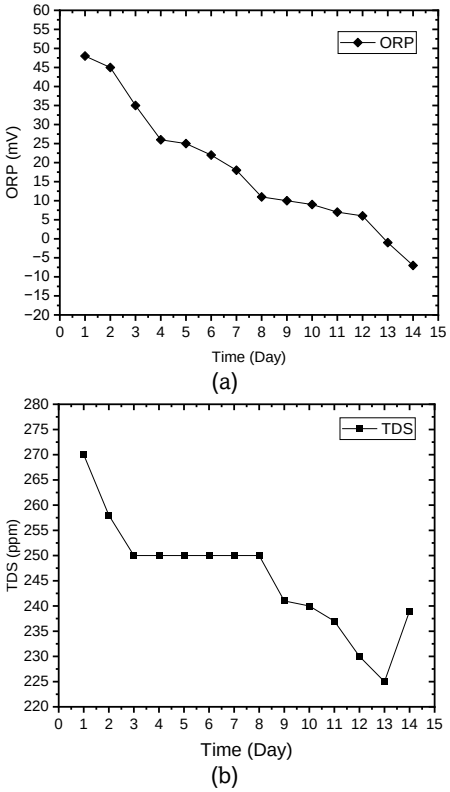

Fig 13. Daily reading of (a) oxidation-reduction potential (ORP), and (b) total dissolved solids (TDS).

This is contrary to the minute changes; the increase in the pH ranges from 7.72 to 8.28, which was about only a 7.3% change in that range. The pH reading was identified as unstable and did not show any significant trends as the trial of wastewater continued. This can be attributed to the instability of the wastewater sample and, thus, is typical for a system with disturbance. This could happen when the set-up is suddenly moved or disturbed.

The highest ORP value was read on the first day at +48.0 mV, and the lowest was read on the last measurement day at -7 mV, as shown in Figure 13. Biochemical reactions such as denitrification may correspond to the results being that these figures were identified to be in between the range of +50 mV to -50 mV in the ORP, wherein the nitrate (NO_3^-) reduction to molecular nitrogen (N_2) in the wastewater sample occurs. Denitrification occurs in an anoxic (no oxygen) environment wherein heterotrophic bacteria are mainly responsible for converting nitrates to nitrogen (Si *et al.,* 2018). This ties nicely with the fact that the MFC design was theoretically targeted to be a closed system and anaerobic, limiting oxygen in the system. This was done by incorporating rubber linings on the lid and the holes atop the lid where the 32 individual MFCs were positioned. However, this would not be tangibly verified since no direct measurements of nitrates and nitrogen content in the system were done. That is part of the limitation of the project. However, in terms of the obtained ORP and pH values measured for 15 consecutive days, together with the TDS, an inversely proportional relationship between the two parameters, pH and ORP, is supported by similar studies (Copeland *et al.,* 2004).

The wastewater's total dissolved solids (TDS) content can be attributed to the dissolved minerals and salts present in the substrate. Shown in Figure 13 was the TDS trend on the 15-day reading. The concentration of the TDS on the first day of the measurement was 270 ppm, which decreased to the lowest concentration of 225 ppm. A similar MFC study aligns with this decrease in TDS and other parameters such as total suspended solids (TSS) and nitrates (NO_3^-), arguing how viable the MFC system is as an economical technology in wastewater treatment. This occurs due to the microorganisms present in the substrate and is impacted by some elements in the sample, such as salt content, wastewater volume, and oxidation and oxygen reduction occurring in the system. There is no direct correlation between the TDS and the other parameters, pH and ORP. However, the researchers noted that the inverse relationship between the data produced by TDS and pH may have been due to some components like phosphates, nitrates, carbonates, minerals, or other impurities present as dissolved solids in the wastewater utilized. These impurities presently affect the chemical properties of the water, wherein the pH changes may happen based on, thus also affecting the ORP. A good example is that pure water with a pH of 7.0 will likely have a negligible value to zero TDS.

3.7. COD Removal Efficiency

The chemical oxygen demand removal and the design of electrodes function in a microbial fuel cell (MFC) system as factors that are usually modified and studied due to their correlation. In essence, the surface area of the electrode is deemed to be a significant factor in increasing its efficiency due to its function as biocatalytic activities happen in these sites. Prior studies have found a correlation between the power densities of microbial fuel cells and COD removal efficiency. A study on an air-cathode MFC using petrochemical wastewater showed that COD removal efficiency and power generation increase (Sarmin *et al.*, 2018). Furthermore, a study on the operation of another air-cathode MFC system utilizing a biofilm and operating at different COD concentrations showed an optimum range of external resistances wherein maximum power is generated. Herein, a comparison of polarization curves of different COD concentrations shows the highest power density generated from the MFC operated with the highest COD concentration (Pinto *et al.,* 2022). This explains the parameter being tested in several MFC systems with various changes in design fabrication and using several wastewater types.

The percent COD removal calculated and achieved by the system is about 95.24% removal efficiency (initial COD of 987 ppm, final COD of 47 ppm). This parameter may be identified to be an integral part and factor of the MFCs' overall efficiency since organic matters that were oxidized by the bacterial activities inside the system while simultaneously producing energy are attributed and quantified through the COD removal efficiency. A similar pattern of results has been found in previous studies wherein the COD removal efficiency of the MFC systems was measured. A study on MFC-cascade stacked using a siphon-type tubing system achieved about 96% COD removal efficiency (Ledezma *et al.*, 2013). Another study of MFCs incorporating dairy wastewater on a dual-chambered system obtained a maximum % COD removal of 92% (Al-saned *et al.,* 2021). Furthermore, the 32-celled MFC study showed a greater COD removal efficiency than another 3D-printed membrane electrode assembly that was fabricated by a graphite coating has achieved <80% COD reduction (Theodosiou *et al.,* 2019) versus the 95% reduction attained in this study. These findings suggest that the 32-celled MFC system can keep up and may even surpass the efficiencies from existing designs of current studies. Moreover, the relationship of the electrode design played a significant role in this bacterial activity. The greater surface area

corresponds to more sites for biocatalytic activities to occur. This is quantified by the COD removal efficiency where organic matter from the wastewater used was consumed while that consumption allows bioelectricity generation (Malik *et al*., 2023). Moreover, nutrient depletion happens when bacterial activities are no longer maintained due to decreased soluble COD, eventually reaching a certain threshold (Li *et al.,* 2021).

4. Conclusion

Incorporating 3D-printing technology in the fabrication of the 32-celled MFC technology offered flexibility on the design freedom with the gyroid pattern appealing to desired electrode properties of bacterial adhesion by increasing its surface area. The study attained a maximum voltage of 633 mV and a current of 14.22 µA from the individual cell reading. The comparison of the pure series and pure parallel cumulative stacking shows the underperformance of the series stacking. It favors the parallel configuration as well as the hybrid parallel configurations to illustrate a more efficient operation than the series. The power and power density data show the maximum attainable power of 11.49 µW and power density of 29.30 µW/m^2 from the pure parallel connection. The higher the current and voltage values with low external resistance, the higher power generated, thus, higher power density. On the contrary, the highest external resistance of 25400 Ω (pure series) gives the least power density of 1.45 µW/m^2. Higher current and voltage values with low external resistance corresponded to higher power generated and, thus, higher power density.

The MPP of the 32-celled MFC system is at the internal resistance of 1369 Ω. Collectively, the results show consistent data favoring the pure cumulative and PS connections over pure series and SP connections. Additionally, wastewater parameters of %COD reduction, pH, TDS, and ORP were measured accordingly. The TDS and ORP collectively decreased over the testing period, possibly attributed to denitrification of the substrate, which was not exclusively covered in this paper. There were minute changes in pH that ranged from 7.72 to 8.28. The %COD reduction of 95.24% efficiency indicates high generation of power densities, and the identification of the range of external resistances from the polarization studies for a particular COD content can be helpful to prevent the decrease in mass transfer losses, eventually leading to a decrease to no current produced. The latter occurs when operating beyond the optimum range of external resistances. The use of diode for hybrid circuits could reduce the effects of voltage reversal during MFCs voltage generation. This could further enhance the capacity of the system to produce more power and efficiency.

References

Abid, A. G., Manzoor, S., Usman, M., Munawar, T., Nisa, M. U., Iqbal, F., Ashiq, M. N., Najam-Ul-Haq, M., Shah, A., & Imran, M. (2021). Scalable synthesis of Sm2O3/Fe2O3 hierarchical oxygen vacancy-based gyroid-inspired morphology: With enhanced electrocatalytic activity for oxygen evolution performance. *Energy and Fuels*, *35*(21), 17820–17832. https://doi.org/10.1021/ACS.ENERGYFUELS.1C01790/ASSET/IMAGES/LARGE/EF1C01790_0009.JPEG

Alonso-Lemus, I. L., Cobos-Reyes, C., Figueroa-Torres, M., Escobar-Morales, B., Aruna, K. K., Akash, P., Fernández-Luqueño, F., & Rodríguez-Varela, J. (2022). Green Power Generation by Microbial Fuel Cells Using Pharmaceutical Wastewater as Substrate and Electroactive Biofilms (Bacteria/Biocarbon). *Journal of Chemistry*, *2022*. https://doi.org/10.1155/2022/1963973

Al-saned, A. J. O., Kitafa, B. A., & Badday, A. S. (2021). Microbial fuel cells (MFC) in the treatment of dairy wastewater. *IOP Conference Series: Materials Science and Engineering*, *1067*(1), 012073. https://doi.org/10.1088/1757-899X/1067/1/012073

An, J., Kim, T., & Chang, I. S. (2016). Concurrent Control of Power Overshoot and Voltage Reversal with Series Connection of Parallel-Connected Microbial Fuel Cells. *Energy Technology*, *4*(6), 729–736. https://doi.org/10.1002/ENTE.201500466

Bian, B., Shi, D., Cai, X., Hu, M., Guo, Q., Zhang, C., Wang, Q., Sun, A. X., & Yang, J. (2018). 3D printed porous carbon anode for enhanced power generation in microbial fuel cell. *Nano Energy*, *44*, 174–180. https://doi.org/10.1016/J.NANOEN.2017.11.070

Browne, M. P., Redondo, E., & Pumera, M. (2020). 3D Printing for Electrochemical Energy Applications. *Chemical Reviews*, *120*(5), 2783–2810. https://doi.org/10.1021/ACS.CHEMREV.9B00783/ASSET/IMAGES/LARGE/CR9B00783_0011.JPEG

Chang, C. C., Kao, W., & Yu, C. P. (2020). Assessment of voltage reversal effects in the serially connected biocathode-based microbial fuel cells through treatment performance, electrochemical and microbial community analysis. *Chemical Engineering Journal*, *397*, 125368. https://doi.org/10.1016/J.CEJ.2020.125368

Christwardana, M., Hadiyanto, H., Motto, S.A., Sudarno, S., Haryani, K. (2020). Performance evaluation of yeast-assisted microalgal microbial fuel cells on bioremediation of cafeteria wastewater for electricity generation and microalgae biomass production *Biomass and Bioenergy*, 139, art. no. 105617 https://doi.org/10.1016/j.biombioe.2020.105617

Copeland, R. C., James, C. N., & Lytle, D. A. (2004). Relationships Between Oxidation-Reduction Potential . *American Water Works Association WQTC Conference*. https://docslib.org/doc/957899/relationships-between-oxidation-reduction-potential

Daniel, D. K., Das Mankidy, B., Ambarish, K., & Manogari, R. (2009). Construction and operation of a microbial fuel cell for electricity generation from wastewater. *International Journal of Hydrogen Energy*, *34*(17), 7555–7560. https://doi.org/10.1016/J.IJHYDENE.2009.06.012

Gajda, I., Greenman, J., & Ieropoulos, I. A. (2018). Recent advancements in real-world microbial fuel cell applications. *Current Opinion in Electrochemistry*, *11*, 78–83. https://doi.org/10.1016/J.COELEC.2018.09.006

Habibul, N., Hu, Y., Wang, Y. K., Chen, W., Yu, H. Q., & Sheng, G. P. (2016). Bioelectrochemical Chromium(VI) Removal in Plant-Microbial Fuel Cells. *Environmental Science and Technology*, *50*(7), 3882–3889. https://doi.org/10.1021/ACS.EST.5B06376/SUPPL_FILE/ES5B06376_SI_001.PDF

Hadiyanto, H., Christwardana, M., & da Costa, C. (2023). Electrogenic and biomass production capabilities of a Microalgae–Microbial fuel cell (MMFC) system using tapioca wastewater and Spirulina platensis for COD reduction. *Energy Sources, Part A: Recovery, Utilization, and Environmental Effects*, 45(2), 3409–3420. https://doi.org/10.1080/15567036.2019.1668085

Hashem, A. (2019). Microbial Fuel Cell (MFC) Application for Generation of Electricity from Dumping Rubbish and Identification of Potential Electrogenic Bacteria. *Advances in Industrial Biotechnology*, *2*(1), 1–8. https://doi.org/10.24966/AIB-5665/100010

Hussain, F., Al-Zaqri, N., Adnan, A. B. M., Hussin, M. H., Oh, S. E., & Umar, K. (2022). Impact of bakery waste as an organic substrate on microbial fuel cell performance. *Sustainable Energy Technologies and Assessments*, *53*, 102713. https://doi.org/10.1016/J.SETA.2022.102713

Jafary, T., Rahimnejad, M., Ghoreyshi, A. A., Najafpour, G., Hghparast, F., & Daud, W. R. W. (2013). Assessment of bioelectricity production in microbial fuel cells through series and parallel connections. *Energy Conversion and Management*, *75*, 256–262. https://doi.org/10.1016/J.ENCONMAN.2013.06.032

Jung, S., & Regan, J. M. (2011). Influence of External Resistance on Electrogenesis, Methanogenesis, and Anode Prokaryotic Communities in Microbial Fuel Cells. *Applied and Environmental Microbiology*, *77*(2), 564. https://doi.org/10.1128/AEM.01392-10

Kim, S., Chae, K. J., Choi, M. J., & Verstraete, W. (2011). Microbial fuel cells: Recent advances, bacterial communities and application beyond electricity generation. *Environmental Engineering Research*, *16*(4), 51–65. https://doi.org/10.4491/EER.2008.13.2.051

Ledezma, P., Greenman, J., & Ieropoulos, I. (2013). MFC-cascade stacks maximise COD reduction and avoid voltage reversal under adverse conditions. *Bioresource Technology*, *134*, 158–165. https://doi.org/10.1016/J.BIORTECH.2013.01.119

Li, D., Shi, Y., Gao, F., Yang, L., Li, S., & Xiao, L. (2021). Understanding the current plummeting phenomenon in microbial fuel cells (MFCs). *Journal of Water Process Engineering*, *40*, 101984. https://doi.org/10.1016/J.JWPE.2021.101984

Logan, B. E., Hamelers, B., Rozendal, R., Schröder, U., Keller, J., Freguia, S., Aelterman, P., Verstraete, W., & Rabaey, K. (2006). Microbial fuel cells: Methodology and technology. In *Environmental Science and Technology* (Vol. 40, Issue 17, pp. 5181–5192). American Chemical Society . https://doi.org/10.1021/es0605016

Lovley, D. R., Ueki, T., Zhang, T., Malvankar, N. S., Shrestha, P. M., Flanagan, K. A., Aklujkar, M., Butler, J. E., Giloteaux, L., Rotaru, A. E., Holmes, D. E., Franks, A. E., Orellana, R., Risso, C., & Nevin, K. P. (2011). Geobacter: The Microbe Electric's Physiology, Ecology, and Practical Applications. *Advances in Microbial Physiology*, *59*, 1–100. https://doi.org/10.1016/B978-0-12-387661-4.00004-5

Malik, S., Kishore, S., Dhasmana, A., Kumari, P., Mitra, T., Chaudhary, V., Kumari, R., Bora, J., Ranjan, A., Minkina, T., & Rajput, V. D. (2023). A Perspective Review on Microbial Fuel Cells in Treatment and Product Recovery from Wastewater. *Water 2023, Vol. 15, Page 316*, *15*(2), 316. https://doi.org/10.3390/W15020316

Mustakeem. (2015). Electrode materials for microbial fuel cells: Nanomaterial approach. *Materials for Renewable and Sustainable Energy*, *4*(4), 1–11. https://doi.org/10.1007/S40243-015-0063-8/FIGURES/9

Oh, S. E., & Logan, B. E. (2007). Voltage reversal during microbial fuel cell stack operation. *Journal of Power Sources*, *167*(1), 11–17. https://doi.org/10.1016/J.JPOWSOUR.2007.02.016

Patrick, M., Malinis, D., Jones, H., Velasco, F., Ray, K., & Pamintuan, S. (2023). Performance evaluation of the novel 3D-printed aquatic plant-microbial fuel cell assembly with Eichhornia crassipes. *International Journal of Renewable Energy Development*, *12*(5), 942–951. https://doi.org/10.14710/IJRED.2023.53222

Pinto, M. F. R., Sofia, V., De Oliveira, B., Das, S., & Calay, R. K. (2022). Experimental Study of Power Generation and COD Removal Efficiency by Air Cathode Microbial Fuel Cell Using Shewanella baltica 20. *Energies 2022, Vol. 15, Page 4152*, *15*(11), 4152. https://doi.org/10.3390/EN15114152

Rahimnejad, M., Adhami, A., Darvari, S., Zirepour, A., & Oh, S. E. (2015). Microbial fuel cell as new technology for bioelectricity generation: A review. *Alexandria Engineering Journal*, *54*(3), 745–756. https://doi.org/10.1016/J.AEJ.2015.03.031

Sarmin, S., Ideris, A., Chin, S. Y., Chin, K. C., & Rahman Khan, Md. M. (2018). PEFORMANCE EVALUATION OF PETROCHEMICAL WASTEWATER FED AIR-CATHODE MICROBIAL FUEL CELLS USING YEAST BIOCATALYST. *Journal of Chemical Engineering and Industrial Biotechnology*, *4*(1), 32–43. https://doi.org/10.15282/JCEIB.V4I1.3881

Si, Z., Song, X., Wang, Y., Cao, X., Zhao, Y., Wang, B., Chen, Y., & Arefe, A. (2018). Intensified heterotrophic denitrification in constructed wetlands using four solid carbon sources: Denitrification efficiency and bacterial community structure. *Bioresource Technology*, *267*, 416–425. https://doi.org/10.1016/J.BIORTECH.2018.07.029

Simeon, M. I., Asoiro, F. U., Aliyu, M., Raji, O. A., & Freitag, R. (2020). *Polarization and power density trends of a soil-based microbial fuel cell treated with human urine*. https://doi.org/10.1002/er.5391

Sonawane, J. M., Mahadevan, R., Pandey, A., & Greener, J. (2022). Recent progress in microbial fuel cells using substrates from diverse sources. *Heliyon*, *8*(12), e12353. https://doi.org/10.1016/J.HELIYON.2022.E12353

Theodosiou, P., Greenman, J., & Ieropoulos, I. (2019). Towards monolithically printed Mfcs: Development of a 3d-printable membrane electrode assembly (mea). *International Journal of Hydrogen Energy*, *44*(9), 4450–4462. https://doi.org/10.1016/J.IJHYDENE.2018.12.163

Wei, J., Liang, P., & Huang, X. (2011). Recent progress in electrodes for microbial fuel cells. *Bioresource Technology*, *102*(20), 9335–9344. https://doi.org/10.1016/J.BIORTECH.2011.07.019

Wu, S., Li, H., Zhou, X., Liang, P., Zhang, X., Jiang, Y., & Huang, X. (2016). A novel pilot-scale stacked microbial fuel cell for efficient electricity generation and wastewater treatment. *Water Research*, *98*, 396–403. https://doi.org/10.1016/J.WATRES.2016.04.043

Xie, X., Hu, L., Pasta, M., Wells, G. F., Kong, D., Criddle, C. S., & Cui, Y. (2011). Three-dimensional carbon nanotube-textile anode for high-performance microbial fuel cells. *Nano Letters*, *11*(1), 291–296. https://doi.org/10.1021/NL103905T/SUPPL_FILE/NL103905T_SI_001.PDF

Yanuka-Golub, K., Dubinsky, V., Korenblum, E., Reshef, L., Ofek-Lalzar, M., Rishpon, J., & Gophna, U. (2021). Anode surface bioaugmentation enhances deterministic biofilm assembly in microbial fuel cells. *MBio*, *12*(2), 1–15. https://doi.org/10.1128/MBIO.03629-20/SUPPL_FILE/MBIO.03629-20-S0001.DOCX

Yazdi, A. A., D'Angelo, L., Omer, N., Windiasti, G., Lu, X., & Xu, J. (2016). Carbon nanotube modification of microbial fuel cell electrodes. *Biosensors and Bioelectronics*, *85*, 536–552. https://doi.org/10.1016/J.BIOS.2016.05.033

You, J., Greenman, J., & Ieropoulos, I. A. (2021). Microbial fuel cells in the house: A study on real household wastewater samples for treatment and power. *Sustainable Energy Technologies and Assessments*, *48*, 101618. https://doi.org/10.1016/J.SETA.2021.101618

You, J., Preen, R. J., Bull, L., Greenman, J., & Ieropoulos, I. (2017). 3D printed components of microbial fuel cells: Towards monolithic microbial fuel cell fabrication using additive layer manufacturing. *Sustainable Energy Technologies and Assessments*, *19*, 94–101. https://doi.org/10.1016/J.SETA.2016.11.006